

## Cross section determination for TAD materials in quasi mono-energetic neutron spectrum from p(Li) reaction

Dusan Kral<sup>1,\*</sup>, Miroslav Zeman<sup>1,2</sup>, Karel Katovsky<sup>1</sup>, Elmira Melyan<sup>1,3</sup>, and Robert Holomb<sup>1,4</sup>

<sup>1</sup>Brno University of Technology, Faculty of Electrical Engineering and Communication, Department of Electrical Power Engineering, Brno, Czech Republic

<sup>2</sup>Joint Institute for Nuclear Research, Dubna, Russian Federation

<sup>3</sup>Chair of Nuclear Physics, Faculty of Physics, Yerevan State University, Yerevan, Republic of Armenia

<sup>4</sup>Department of Nuclear Physics and Elementary Particles, Uzhhorod National University, Uzhhorod, Ukraine

**Abstract.** Threshold activation detectors (TAD) are of great importance for a determination of neutron energy spectra and flux density. For different sources, it is necessary to choose the right combination of materials that cover the estimated spectra. Several different materials were irradiated in a quasi-monoenergetic neutron field with 29.1 MeV peak neutrons energy in the CANAM facility. Neutrons were produced in p + Li-7 reaction in a thin target and the foils were situated in the proton beam axis and close geometry to the Li target. The integral number of protons was established from accelerator telemetry and lithium target activation measurements after the experiment. During the experiment, one long irradiation was done for following foils: Al, Au, Bi, Co, Cu, Fe, In, Mn, Pb, Ta, V, Y and four short irradiations for foils: Cu, Fe, In, Ta, V, W, Y. The foils were irradiated in a sandwich configuration, sorted by cross-section where the materials with higher cross-section were placed in the back of the sandwich. Neutrons produced in the p + Li-7 reaction have a quasi mono-energetic spectrum which provides a suitable basis for cross-section determination. Experimental results were calculated for (n,xn), (n,p) and (n, $\alpha$ ) reactions via the dosimetry foils activation method including a gamma-ray spectroscopy method. Several important spectroscopic corrections have to be applied to increase the accuracy of the obtained results, including neutron background suppression. Experimental data will be submitted to the EXFOR database.

### 1 Introduction

Well known cross-sections for different neutron reactions are important for most nuclear applications. Some reactions are described from low energy to high energies, but most of them do not have enough experimental data. One of the applications that need a good knowledge of the cross-sections is measuring of a neutron flux density and neutron spectrum with the TAD. This off-line method uses a difference in energy of thresholds for various nuclear reactions. For spectrum with energy from several hundred keV up to several MeV are important (n,p), (n,n'), and (n, $\alpha$ ). An (n,xn) reactions are used from several MeV up to dozens of MeV. The use of TAD is wide for example the describing neutron field around some experimental set-ups, channels, and different devices. The TAD main advantages are simple usage, small dimensions, low cost, and with a large number of detectors is possible to make very accurate measurement during one irradiation.

### 2 Experimental part

The experimental part was carried out at the Center of Accelerators and Nuclear Analytical Methods (CANAM), Nuclear Physics Institute (NPI) of the Czech Academy

\*e-mail: xkrald00@vutbr.cz

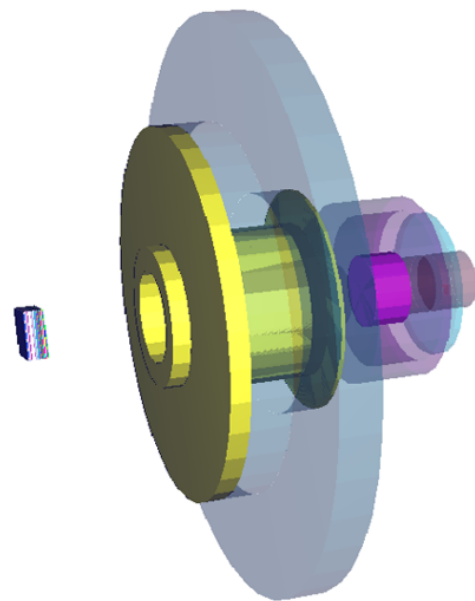


**Figure 1.** MCNPX model of lithium target with samples.

of Science in Rez, Czech Republic. Experimental samples were irradiated by the quasi-monoenergetic spectrum from lithium neutron source [1]. Neutrons are produced

in  ${}^7\text{Li}(p,n){}^7\text{Be}$  reaction. The measurement was done with energy 29.1 MeV in neutron peak. All the samples had the same dimension  $1.25 \times 1.25 \text{ cm}^2$  with different thicknesses. The weights of the samples vary from 0.1 to 0.7 g depending on the values of cross-sections of expected reactions. The foils were mounted on an aluminum holder in sandwich in this order: V, Ta, Y, Fe, Al, Cu, Mn, Co, Bi, In, Pb and Au. The nuclear reactions from a gold sample were used as a neutron fluence monitor. All samples were in high purity metallic form. Figure 1 shows 3D model of samples in sandwich behind the neutron source [2]. The irradiation took 8 hours and proton beam intensity was around  $6 \mu\text{A}$ . After the end of irradiation, the samples were measured at HPGe detectors at NPI in Rez, the University of Defence in Vyskov, and at BUT in Brno. Each sample was measured several times with a different time of measurement.

### 3 Cross section calculations

The spectra from gamma spectroscopy measurement were processed in Deimos32 software [3]. Due to the high amount of experimental data were all the gamma spectrometric correction applied in special software packages [4]. The output from code is a production rate for each isotope and decay curve reconstructed from the individual measurement. Production rate is calculated by this equation

$$Q = S(E_\gamma) \frac{1}{t_{live}} \frac{1}{I_\gamma(E_\gamma)} \frac{\lambda t_{real}}{1 - e^{-\lambda t_{real}}} \cdot \frac{1}{1 - e^{-\lambda t_{irr}}} \frac{1}{e^{-\lambda t_{delay}}} \frac{C_{abs}}{\varepsilon_{FEP}(E_\gamma) \cdot COI_E}, \quad (1)$$

where  $S(E_\gamma)$  is peak area of gamma line,  $I_\gamma$  is the intensity of gamma line,  $\lambda$  is the decay constant,  $t_{real}$  is the real measurement time,  $t_{live}$  is the live time of the measurement,  $t_{irr}$  is the length of irradiation and  $t_{delay}$  is the time between the end of the irradiation and beginning of the measurement.  $\varepsilon_{FEP}$  is the full energy-peak efficiency,  $C_{abs}$  is the self-absorption correction and  $COI_E$  is the correction for true coincidence summing.

The correction for true coincidence summing was obtained from TrueCoinc code [5]. This negative effect applies to close measurements on the HPGe detector. Due to the high relative efficiency of detectors in Rez was not necessary to use this correction on the data from NPI. The accuracy in correction determination is influenced by the calculation of both a total and full-energy-peak efficiency.

The final cross-section from the production rate was calculated by this equation

$$\sigma = \frac{Q \cdot S \cdot C_{bg}}{\frac{N_n}{t_{irr}} C_{flux} \frac{N_A \cdot m \cdot r}{A_r}}, \quad (2)$$

where  $S$  is the sample surface perpendicular to proton beam,  $N_n$  is the neutron fluence,  $m_s$  is the sample weight,  $A_r$  is the relative atomic mass of the sample,  $N_A$  is the Avogadro constant,  $r$  is the abundance of isotopes of a chemical element,  $C_{bgr}$  is the background correction, which

refers to a part of neutron spectrum outside the peak and  $C_{flux}$  is a correction of neutron flux intensity [6].

The value of neutron fluence was calculated from the production rate of (n,2n), (n,3n), and (n,4n) reaction in gold foil with the same equation as 2. This is possible due to good knowledge of gold cross-sections in this energy range.

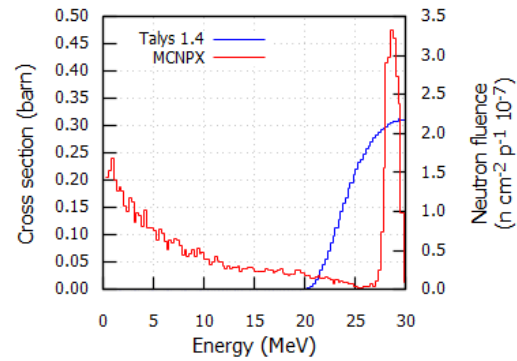


**Figure 2.** Neutron spectrum and cross section for  ${}^{59}\text{Co}(n,3n)$  reaction.

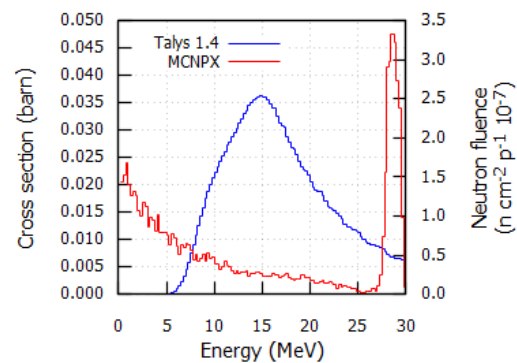


**Figure 3.** Neutron spectrum and cross section for  ${}^{59}\text{Co}(n,\alpha)$  reaction.

#### 3.1 Background subtraction and neutron flux correction

The quasi-monoenergetic spectrum from the neutron source has a monoenergetic peak and continuum at lower energies. The contribution of those lower energies could be half of the flux intensity with respect to the proton energy. Therefore it is necessary to subtract this background for all reactions in which threshold energy is much lower than the energy of neutron peak.

Subtraction is based on the calculated cross-section from Talys 1.4 [7] and simulated neutron spectrum from MCNPX [8]. The Talys 1.4 was used and verified for this type of measurement in older experiments and works [6, 9]. The correction factor is calculated as a ratio between a product of cross-section and neutron flux in peak and for the whole spectrum [6]. The background subtraction process is independent of an absolute value of cross-section. It depends only on the shape of the cross-section.

The main advantage of the Talys code is the ability to simulate cross-sections for high energies for which evaluated data are not available. Also for less typical reactions that do not have any available data.

Because both spectra are binned with step 250 keV the correction formula has this form

$$C_{bgr} = \frac{\sum_{i,peak} \sigma_i \cdot N_i}{\sum_{i,spectrum} \sigma_i \cdot N_i} \quad (3)$$

The neutron flux is simulated for every sample. Two examples of cross section with different energy threshold are shown in Figure 3 and 2. Values of background correction coefficients are in Table 1.

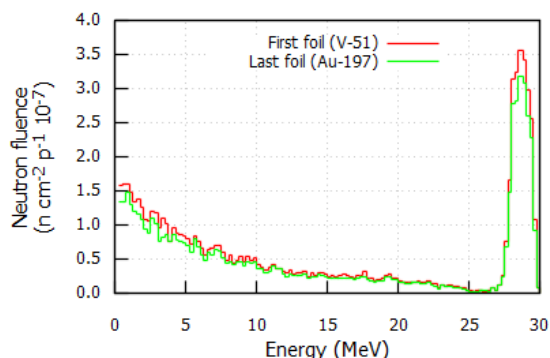


**Figure 4.** Neutron flux comparison.

Because of the intensity of neutron flux decrease with the inverse-square law so it was made neutron flux intensity correction as a ratio between simulated flux in gold foil and the other foils. Neutron flux in the first and last foil is compared in Figure 4. The difference between those two foils is 12 %.

The uncertainty estimation of background subtraction is a sum of simulated neutron spectra uncertainty and uncertainty of the used cross-sections under the neutron peak. The estimation varies for different reactions because some cross-sections are more known than others but none of the uncertainty is greater than 10 % [9]. The background and flux corrections are given in Table 1.

## 4 Results

All the evaluated data are in Table 1. Some of the calculated cross sections are already known and this experiment helps to verify them. The example is  $^{59}\text{Co}(n,\alpha)^{56}\text{Mn}$  reaction which is shown in Figure 5. For some reactions were obtained completely new results. Those results are shown in Figures 6 and 7. In all plots are results compared with current data from the EXFOR database, simulated cross-sections from Talys 1.4 code, and with some available evaluated data like EAF-2010 [10] or BROND-3.1 [11].

## 5 Conclusion

The quasi-monoenergetic neutron source was used to obtain (n,xn), (n,α) and (n,p) cross sections for these ma-

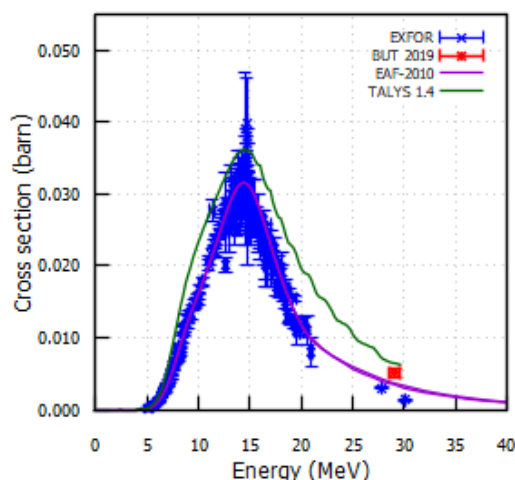


**Figure 5.** Cross-section for  $^{59}\text{Co}(n,\alpha)^{56}\text{Mn}$  reaction.

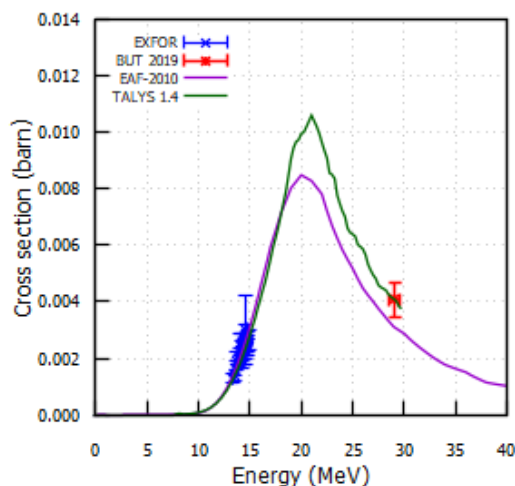


**Figure 6.** Cross-section for  $^{115}\text{In}(n,\alpha)^{112}\text{Ag}$  reaction.

terials: V, Ta, Y, Fe, Al, Cu, Mn, Co, Bi and In for the energy 29.1 MeV. Uncertainties of calculated values are caused by neutron fluence calculation, background correction, and spectroscopic analysis. Most of the uncertainties are near 15 %. Obtained data are in good agreement with theoretical and experimental data.

Some results are completely new for this energy and will be helpful to verify theoretical models and applications that use nuclear data. The difference between obtained data and well-known cross-section will be subject of further analysis during the processing of new measurements with different neutron energy.

## Acknowledgement

All measurements were carried out at the CANAM infrastructure of the NPI CAS Rez supported through MŠMT project No. LM2015056. Also, we would like to thank all the staff who helped with the preparation and execution of those measurements.

**Table 1.** Cross section results

Isotope (-)	Abundance (%)	Reaction (-)	$E_{th}$ (MeV)	$T_{1/2}$	$C_{flux}$ (-)	$C_{bg}$ (-)	XS (barn)	dXS (barn)
$^{27}\text{Al}$	100	(n, $\alpha$ )	3.25	14.958 h	1.03	0.15	0.0027	0.0004
$^{51}\text{V}$	99.75	(n, $\alpha$ )	2.10	43.67 h	1.00	0.40	0.0060	0.0009
$^{56}\text{Fe}$	91.72	(n,p)	2.97	2.57878 h	1.02	0.26	0.0266	0.0038
$^{55}\text{Mn}$	100	(n,2n)	10.40	312.19 d	1.05	0.46	0.2069	0.0295
$^{59}\text{Co}$	100	(n, $\alpha$ )	0.00	2.57878 h	1.07	0.25	0.0051	0.0007
$^{59}\text{Co}$	100	(n,p)	0.80	44.494 d	1.07	0.29	0.0172	0.0025
$^{59}\text{Co}$	100	(n,2n)	10.60	70.85 d	1.07	0.47	0.2594	0.0371
$^{59}\text{Co}$	100	(n,3n)	19.35	271.81 d	1.07	0.96	0.2752	0.0393
$^{63}\text{Cu}$	69.17	(n,3n)	22.67	3.366 h	1.04	0.98	0.1364	0.0275
$^{65}\text{Cu}$	30.83	(n,p)	1.38	2.5172 h	1.04	0.47	0.0128	0.0019
$^{89}\text{Y}$	100	(n, $\alpha$ )	0.00	18.631 d	1.02	0.68	0.0066	0.0011
$^{89}\text{Y}$	100	(n,2n)	11.61	106.63 d	1.02	0.50	0.4946	0.0703
$^{89}\text{Y}$	100	(n,3n)	21.10	79.8 h	1.02	0.98	0.7066	0.1008
$^{89}\text{Y}$	100	(n,3n)-m	21.10	13.37 h	1.02	0.98	0.4548	0.0647
$^{115}\text{In}$	95.70	(n,n')-m	0.00	4.486 h	1.12	0.06	0.0372	0.0053
$^{115}\text{In}$	95.70	(n, $\alpha$ )	0.00	3.13 h	1.12	0.62	0.0041	0.0006
$^{115}\text{In}$	95.70	(n,2n)-m	9.10	49.51 d	1.12	0.33	0.3571	0.0511
$^{209}\text{Bi}$	100	(n,4n)	22.55	6.243 d	1.09	1.00	0.8280	0.1180

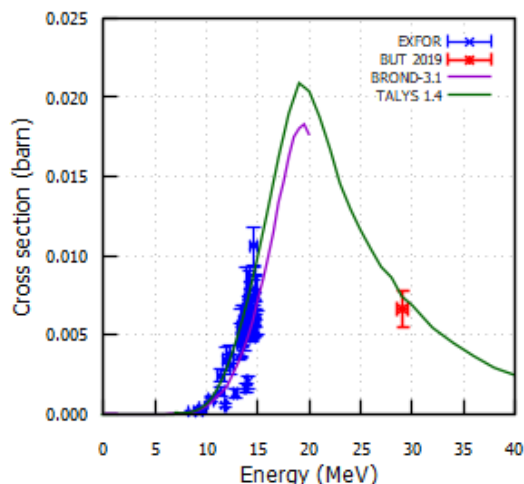


**Figure 7.** Cross-section for  $^{89}\text{Y}(n,\alpha)^{86}\text{Rb}$  reaction.

Authors gratefully acknowledge financial support from the Ministry of Education, Youth and Sports of the Czech Republic under Brno University of Technology specific research program (project No. FEKT-S-17-4784 “New Technologies for sustainable power engineering”)

Authors thank Mr. Jiri Janda for providing detectors at the University of Defense in Vyskov, which were important for the precise measurement of activated foils.

## References

[1] P. Bém, V. Burjan, J. Dobeš, U. Fischer, M. Götz, M. Honusek, V. Kroha, J. Novák, S.P. Simakov,

E. Šimečková, *The NPI cyclotron-based fast neutron facility*, in ND2007 (EDP Sciences, 2007)

[2] R. Schwarz, L. Carter, Transactions of the American Nuclear Society **77** (1997)  
 [3] J. Frana, Journal of Radioanalytical and Nuclear Chemistry **257**, 583 (2003)  
 [4] J. Adam, J. Mrazek, J. Frana, A. Balabekyan, V. Pronskikh, V. Kalinnikov, A. Priemyshev, Measurement Techniques **44**, 93 (2001)  
 [5] S. Sudár, IAEA Tecdoc **1275**, 37 (2002)  
 [6] J. Vrzalová, O. Svoboda, A. Krása, A. Kugler, M. Majerle, M. Suchopár, V. Wagner, Nuclear Instruments and Methods in Physics Research Section A: Accelerators, Spectrometers, Detectors and Associated Equipment **726**, 84 (2013)  
 [7] A.J. Koning, D. Rochman, S. van der Marck, J. Kopecky, J.C. Sublet, S. Pomp, H. Sjostrand, R. Forrest, E. Bauge, H. Henriksson et al., Database available from <http://www.talys.eu/tendl-2012> (2014)  
 [8] D.B. Pelowitz et al., *MCNPX user's manual Version 2.7.0* (2011)  
 [9] P. Chudoba, S. Kilim, V. Wagner, J. Vrzalova, O. Svoboda, M. Majerle, M. Stefanik, M. Suchopar, A. Kugler, M. Bielewicz et al., Physics Procedia **59**, 114 (2014)  
 [10] J.C. Sublet, L. Packer, J. Kopecky, R. Forrest, A. Koning, D. Rochman, EASY Documentation Series, CCFE (2010)  
 [11] A. Blokhin, E. Gai, A. Ignatyuk, I. Koba, V. Manokhin, V. Pronyaev, Yad. Reak. Konst **2**, 62 (2016)